

Improved thermal reliability in base contact of full 3-inch InP Double-HBTs with f_T and f_{max} in excess of 300 GHz

In-Geun Lee¹, Yong-Soo Jeon¹, Yonghyun Kim², Jacob Yun², Ted Kim², Hyuk-Min Kwon³, Seung Heon Shin³, Jae-Hak Lee¹, Kyunghoon Yang⁴ and *Dae-Hyun Kim¹

Tel.: +82-(53)-950-7844 E-mail address: dae-hyun.kim@ee.knu.ac.kr

¹School of Electronic and Electrical Engineering, Kyungpook National University, Daegu, 41566, South Korea

²QSI, Cheon-An, Chungcheongnam-do, 31044, South Korea

³Semiconductor Convergence Campus, Korea Polytechnics, Anseong-si, 17550, South Korea

⁴School of Electrical Engineering, Korea Advanced Institute of Science and Technology, Daejeon, 34141, South Korea

Keywords: Double heterojunction bipolar transistors (DHBTs), Cut-off frequency (f_T), maximum oscillation frequency (f_{max}), Indium phosphide (InP), Thermal stress

Abstract

In this paper, we have structurally and electrically examined the thermal degradation of platinum-based ohmic contacts for base layers of InP DHBTs. The results show that the degradation of the base contact is caused by the formation of an inhomogeneous Au-InGaAs alloy. It was also found that the contact resistance degradation could be effectively suppressed by inserting a molybdenum diffusion barrier. We demonstrate an InP DHBT on a 3-inch InP substrate via stepper-based photolithography with an improved base ohmic contact. The fabricated DHBTs ($W_E = 1.0 \mu\text{m}$ and $L_E = 15 \mu\text{m}$) exhibit high current gain (β) = 57 at $V_{CE} = 1.0 \text{ V}$. Excellent f_T of 331 GHz and f_{max} of 310 GHz are obtained at $J_C = 3.2 \text{ mA}/\mu\text{m}^2$ and $V_{CE} = 1.4 \text{ V}$.

INTRODUCTION

As predicted by Edholm's law, wireless data rates have doubled every 18 months over the past three decades [1]. The evolving sixth-generation (6G) wireless communication technologies will demand higher operating frequencies of around 300 GHz with data rates approaching 0.1 Tbps [2-3]. InP double-heterojunction bipolar transistors (DHBTs) are promising for 6G communication technologies because of their potential to reach a maximum oscillation frequency (f_{max}) beyond 1 THz while maintaining a relatively high breakdown voltage [4-6].

The DHBT's capability to drive a high density of current leads to significant heat generation within the device, posing a possible risk to its reliability. In InP DHBTs, non-alloyed ohmic contacts using relatively thermally stable materials have been widely studied for the emitter and collector contacts interfacing with n-type InGaAs, but for the base contact interfacing with p-type InGaAs, Pt- or Pd-based alloyed ohmic contacts are commonly used [7-8], which are more vulnerable to thermal stress. In this work, we aimed to improve the thermal reliability of the base contact by inserting a Mo diffusion barrier. The fabricated DHBTs on a 3-inch InP

substrate exhibited improved thermal reliability of the base ohmic contact resistance, together with both f_T and f_{max} in excess of 300 GHz.

FABRICATION PROCESS

Fig. 1 (a) shows the epitaxial structure of the InP DHBT. All epitaxial layers are grown on a semi-insulating 3-inch InP substrate using molecular-beam epitaxy (MBE). The epitaxial wafer includes n+ InP layers for the emitter and collector and p+ InGaAs layers for the base. At the emitter-base (EB) and base-collector (BC) heterojunctions, chirped-superlattice (CSL) grading (InGaAs/InAlAs) is used to smooth conduction band discontinuities [9].

Device fabrication included electroplating-based emitter contacts, SiN_x sidewall spacers, self-aligned base contacts, and BCB-based interconnections. The detailed process flow is shown in Fig. 1 (b).

Additionally, a TLM test structure was fabricated to investigate thermal stability of the base-contact. TLM devices were fabricated by depositing two different metal stacks (sample-a: Pt/Ti/Pt/Ti/Au = 100/100/100/100/1100 Å, sample-b: Pt/Ti/Mo/Ti/Au = 100/100/100/100/1100 Å) on

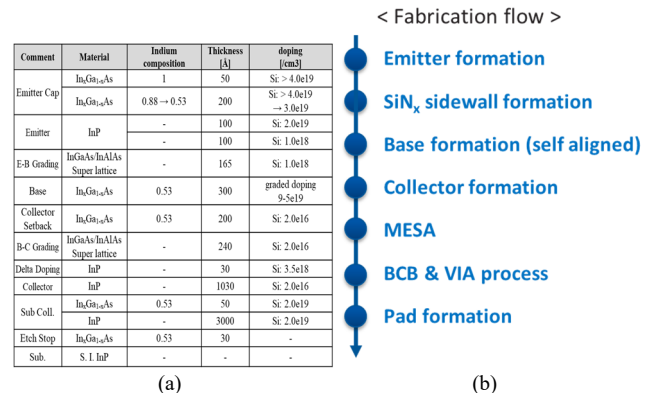


Fig. 1. InP DHBT (a) epitaxial layer structure and (b) fabrication process.

100 nm-thick p-type InGaAs with the same composition and doping concentration as the base layer of the InP DHBT. Subsequently, electrical and structural changes after annealing at 250 °C in N₂ ambient were investigated.

RESULTS AND DISCUSSION

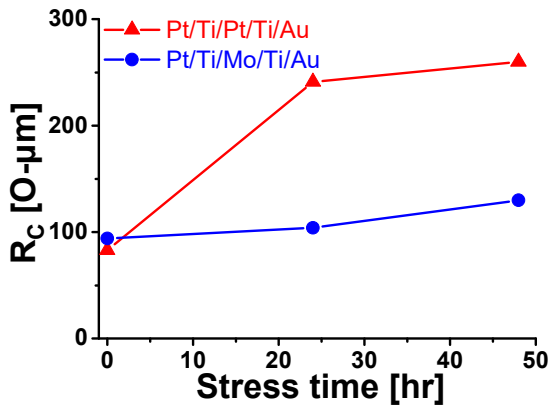


Fig. 2. TLM measurement for Pt/Ti/Pt/Ti/Au (sample-a) and Pt/Ti/Mo/Ti/Au (sample-b) contacts on p⁺ InGaAs at various annealing times.

The graph in Fig. 2 shows the change in contact resistance for the two TLM samples as a function of annealing time. Before annealing, the samples showed similar contact resistance of 83 ohm·μm (sample-a) and 94 ohm·μm (sample-b). For sample-a, the contact resistance increased significantly to 240 and 260 ohm·μm after 24 and 48 hours of annealing, respectively. However, the change in contact resistance for sample-b was insignificant in comparison.

To analyze the difference in thermal stability for the two samples, cross-sectional TEM analysis was performed. Fig. 3 (a) and (b) shows the cross-sectional TEM images for the two samples after 48 hours of annealing. It can be seen for sample-a that Au diffused to the InGaAs layer and formed an inhomogeneous alloy, while in sample-b, only Pt-InGaAs alloy was formed to make ohmic contact and the diffusion of Au was suppressed. From this, it can be seen that the deterioration of the ohmic contact properties of sample-a due to heat is caused by the formation of an inhomogeneous Au-InGaAs alloy, and it is also shown that the insertion of a thin

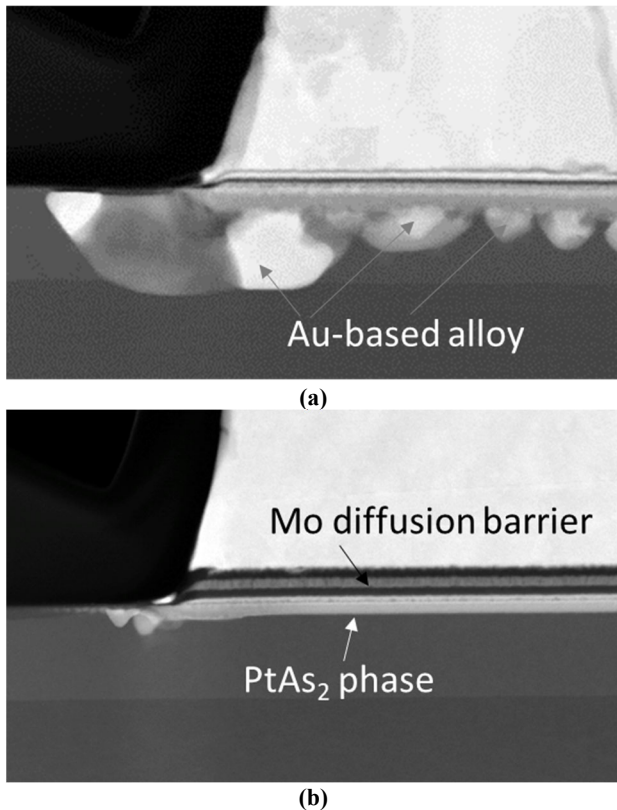


Fig. 3. Cross-sectional TEM images for sample-a (Pt/Ti/Pt/Ti/Au) and sample-b (Pt/Ti/Mo/Ti/Au).

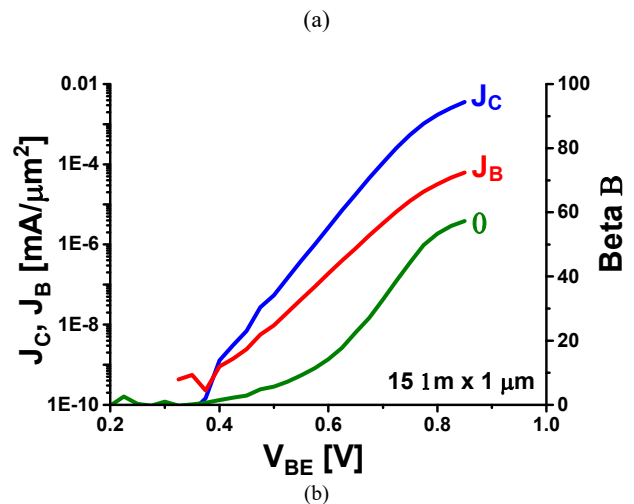


Fig. 4. DC characteristic of the fabricated DHBTs with $W_E = 1 \mu\text{m}$ and $L_E = 15 \mu\text{m}$ (a) Common-emitter IV curves for I_B range from 1 μA to 161 mA (b) Gummel characteristics at $V_{CE} = 1.0 \text{ V}$

molybdenum diffusion barrier can effectively prevent the formation of such an Au-InGaAs alloy.

Fig. 4 shows the DC characteristics of the fabricated DHBTs with $W_E = 1.0 \mu\text{m}$ and $L_E = 15 \mu\text{m}$. The common-emitter IV characteristics of fabricated InP DHBTs as shown in Fig. 4 (a) exhibit high on-current density (J_C) of $6.9 \text{ mA}/\mu\text{m}^2$ at $I_B = 1.61 \text{ mA}$. The excellent current gain (β) = 50 of the fabricated DHBT is obtained from the Gummel characteristics at $V_{CE} = 1 \text{ V}$ as shown in Fig. 4 (b).

To investigate the high-frequency performance, the scattering-parameters (S-parameters) of the fabricated DHBTs were measured from 1 to 50 GHz. The measured high-frequency characteristics, including unity current gain cutoff frequency (f_T) of 331 GHz and maximum oscillation frequency (f_{max}) of 310 GHz at $V_{CE} = 1.4 \text{ V}$ and $J_C = 3.2 \text{ mA}/\mu\text{m}^2$, obtained by extracting pad parasitic elements, are shown in Fig. 5. Thanks to the short base-emitter distance along with process optimization, the devices exhibit high-frequency performance for relatively large area with $W_E = 1.0 \mu\text{m}$ and $L_E = 15 \mu\text{m}$.

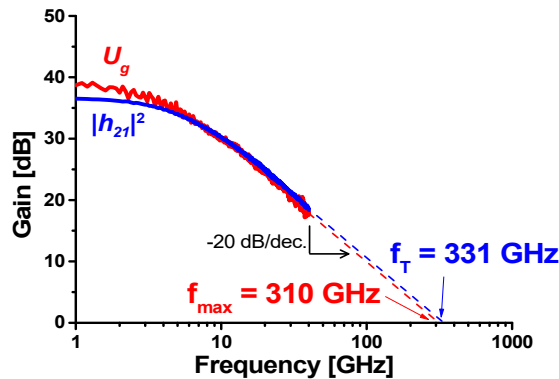


Fig. 5. RF gains ($|h_{21}|^2$ and U_g) vs. frequency for the fabricated DHBTs with $W_E = 1 \mu\text{m}$ and $L_E = 15 \mu\text{m}$.

CONCLUSIONS

In this work, we have successfully accomplished the optimization of the InP DHBTs process utilizing an i-line stepper. We also investigated the thermal degradation mechanism of a Pt-based ohmic contact for p-type InGaAs and found that the degradation can be suppressed by inserting a thin molybdenum diffusion barrier layer. Additionally, the fabricated InP DHBTs, even with large W_E of $1.0 \mu\text{m}$ and long L_E of $15 \mu\text{m}$, show a high gain (β) of 57 and well-balanced high-frequency characteristics of f_T/f_{max} of 331/310 GHz.

ACKNOWLEDGEMENTS

This work was supported by the National Research and Development Program through the National Research Foundation of Korea (NRF) funded by the Ministry of Science and ICT under Grant 2022M3I8A1078437.

REFERENCES

- [1] S. Cherry, "Edholm's law of bandwidth," *IEEE Spectr.*, vol. 41, no. 7, pp. 58–60, 2004.
- [2] M. Amakawa *et al.*, *White Paper on RF enabling 6G—opportunities and challenges from technology to spectrum*, no. 13. University of Oulu, 2021.
- [3] M. Ikram, K. Sultan, M. F. Lateef, and A. S. M. Alqadami, "A Road towards 6G Communication-A Review of 5G Antennas, Arrays, and Wearable Devices," *Electronics*, vol. 11, no. 1, 2022.
- [4] M. Urteaga, Z. Griffith, M. Seo, J. Hacker, and M. J. W. Rodwell, "InP HBT Technologies for THz Integrated Circuits," *Proceedings of the IEEE*, vol. 105, no. 6, pp. 1051–1067, 2017, doi: 10.1109/JPROC.2017.2692178.
- [5] Y. Shiratori, T. Hoshi, M. Ida, E. Higurashi, and H. Matsuzaki, "High-Speed InP/InGaAsSb DHBT on High-Thermal-Conductivity SiC Substrate," *IEEE Electron Device Letters*, vol. 39, no. 6, pp. 807–810, 2018, doi: 10.1109/LED.2018.2829531.
- [6] S. Kang, D. Kim, M. Urteaga, and M. Seo, "State-of-the-art THz integrated circuits in InP HBT technologies," in *2017 IEEE International Symposium on Radio-Frequency Integration Technology (RFIT)*, 2017, pp. 25–27.
- [7] J. S. Yu, S. H. Kim, and T. I. Kim, "PtTiPtAu and PdTiPtAu ohmic contacts to p-InGaAs," in *Compound Semiconductors 1997. Proceedings of the IEEE Twenty-Fourth International Symposium on Compound Semiconductors*, 1997, pp. 175–178. doi: 10.1109/ISCS.1998.711608.
- [8] J. C. Lin, S. Y. Yu, and S. E. Mohney, "Characterization of low-resistance ohmic contacts to n- and p-type InGaAs," *J Appl Phys*, vol. 114, no. 4, p. 44504, Jul. 2013, doi: 10.1063/1.4816097.
- [9] C. Nguyen, T. Liu, M. Chen, H.-C. Sun, and D. Rensch, "AllInAs/GaInAs/InP double heterojunction bipolar transistor with a novel base-collector design for power applications," *IEEE Electron Device Letters*, vol. 17, no. 3, pp. 133–135, 1996, doi: 10.1109/55.485191.